

Developmental Cell

Supplemental Information

Stable Force Balance between Epithelial Cells

Arises from F-Actin Turnover

Jeanne N. Jodoin, Jonathan S. Coravos, Soline Chanet, Claudia G. Vasquez, Michael Tworoger, Elena R. Kingston, Lizabeth A. Perkins, Norbert Perrimon, and Adam C. Martin

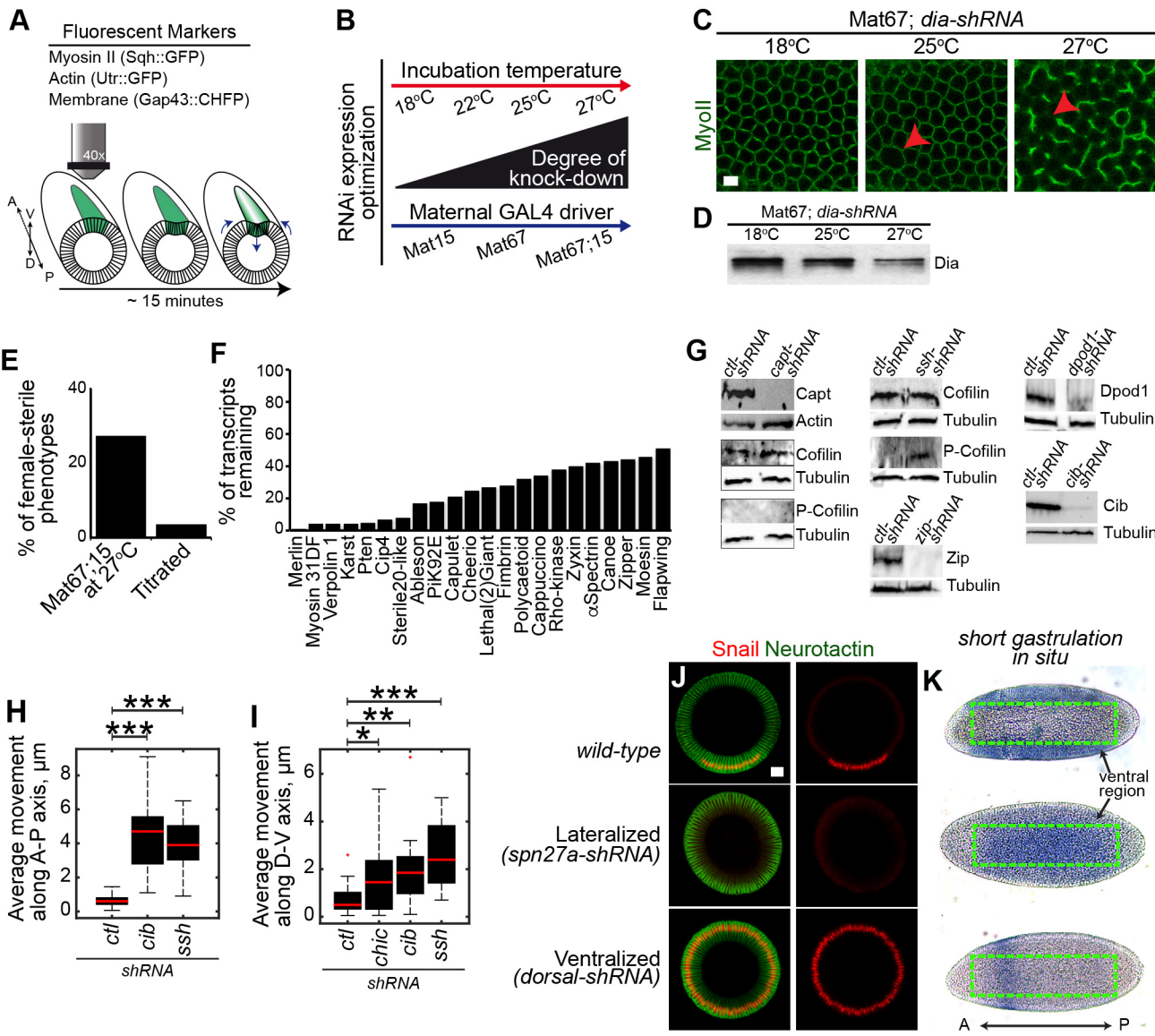
Figure S1

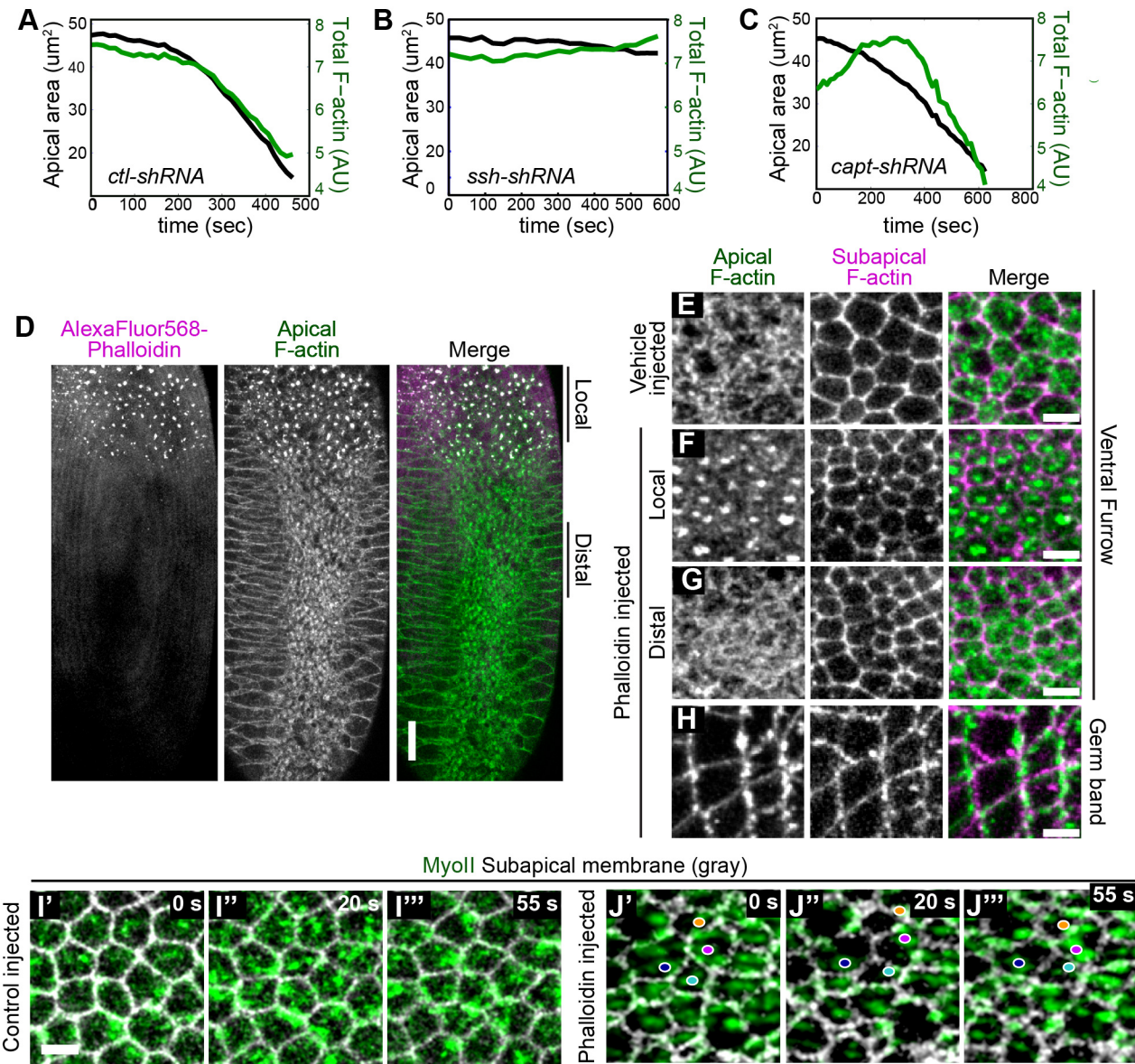
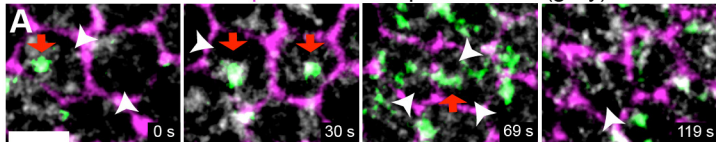
Figure S2

Figure S3

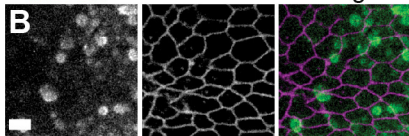
ROCK Subapical F-actin Apical F-actin (gray)



Supra-apical
Moesin

Subapical
Moesin

Merge



Blebs

Actual

Random

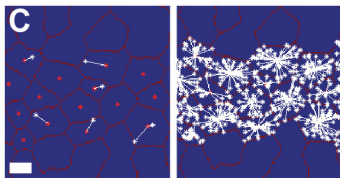


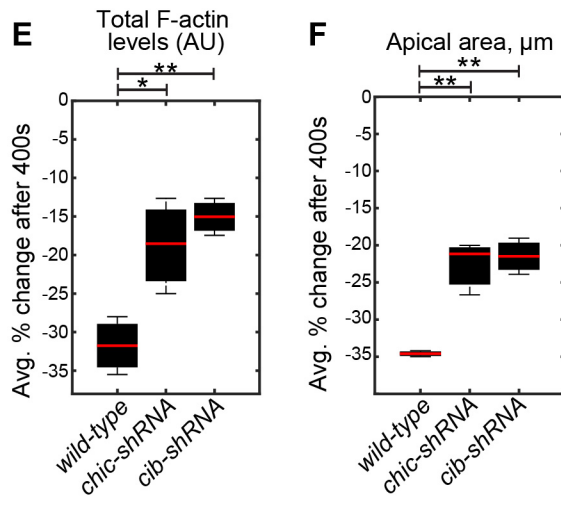
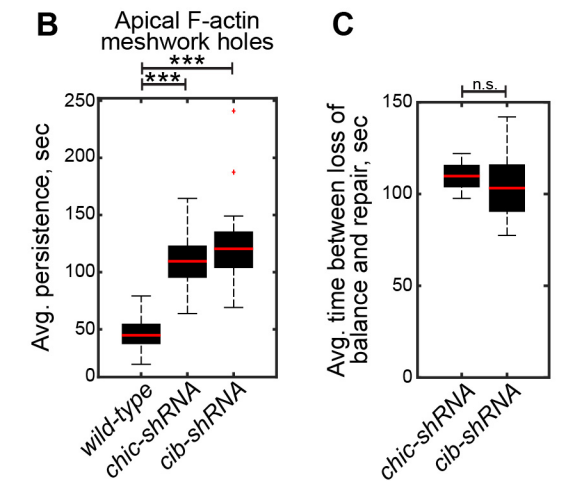
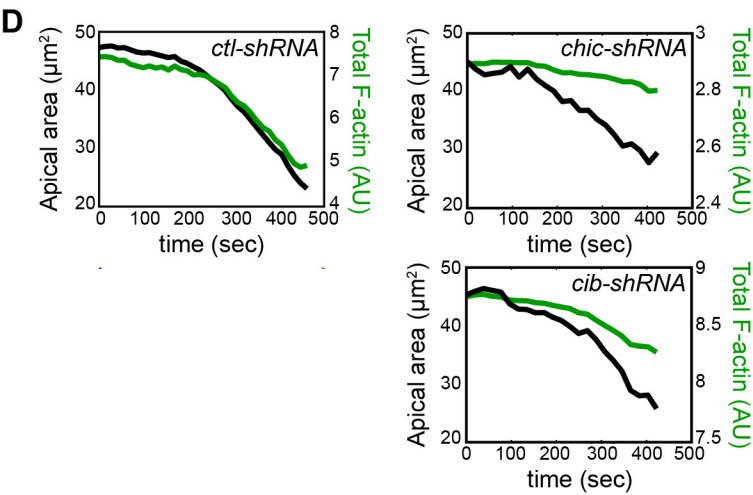
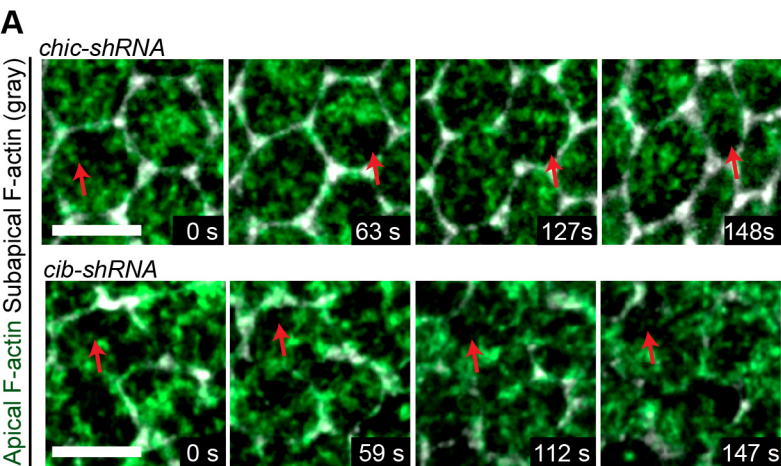
Figure S4

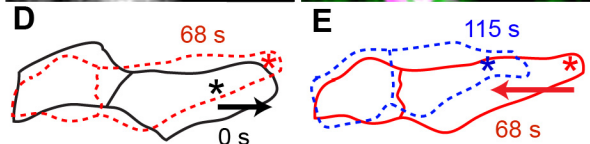
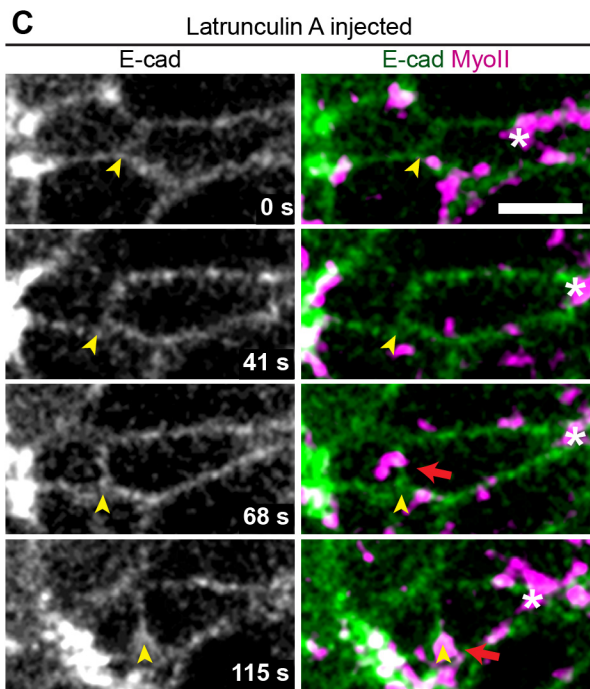
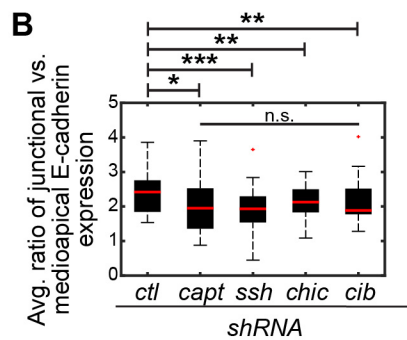
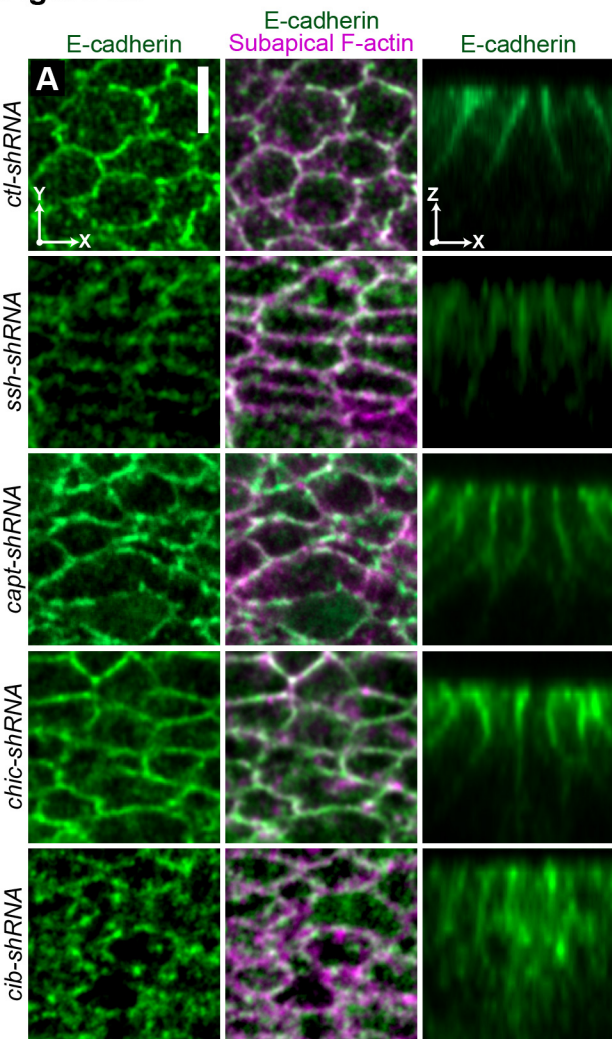
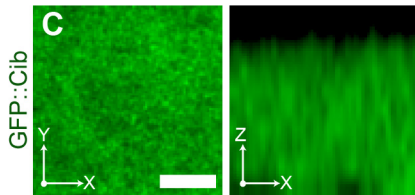
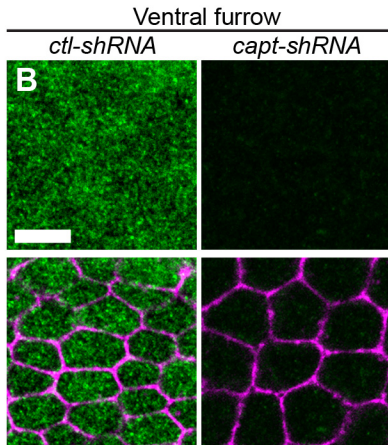
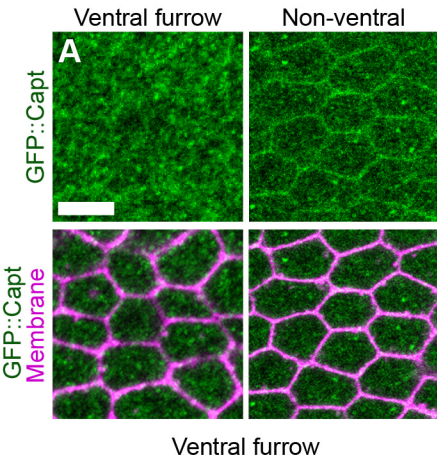
Figure S5

Figure S6



SUPPLEMENTAL FIGURE LEGENDS

Figure S1. RNAi Screen Identifies Requirement of Force Balance During Apical Constriction, Related To Figures 1 and 2. (A) Schematic of live-embryo imaging RNAi screen. UAS-shRNA expression was driven by GAL4 drivers expressing fluorescent markers. Ventral furrow formation was imaged using membrane and cytoskeleton markers. (B) Varying incubation temperature and/or GAL4 driver strength titrates the degree of knockdown for individual genes. (C and D) Degree of *dia* knock-down is influenced by incubation temperature. (C) Disruption of Sqh::GFP (MyoII) localization to basal furrow canals (red arrowhead) is more severe when dia-shRNA is driven at a higher temperature. Scale bars; 5 μ m. (D) Immunoblotting of *dia*-shRNA embryo lysates show that higher incubation temperatures result in the greater decrease in Dia protein levels. (E) Percent of female sterile UAS-shRNA lines at most severe knock down condition (Mat67;15 at 27°C). Female sterility is decreased by titrating the degree of knock-down. (F and G) Validation of UAS-shRNA mediated depletion of indicated transcripts via qPCR (F) or proteins via immunoblotting of RNAi lysates (G). (H and I) F-actin turnover is required for force balance along the A-P and D-V axes in ventral furrow cells. Box and whisker plot of individual MyoII structure movement in the A-P axis (H) and D-V axis (I) following indicated gene depletions. Loss of F-actin turnover results in greater movement along both axes. *** $p < 0.00001$, ** $p < .001$, * $p < .01$ n=3 embryos, ~20 MyoII structures per condition. (J) Representative cross-sections of embryos expressing indicated UAS-shRNA stained for Snail (ventral cell fate, red) and Neurotactin (membranes, green). Snail expression around the entire embryo circumference confirms expansion of ventral region in *spn27a*-shRNA embryos. Scale bar, 10 μ m. (K) *In situ* staining for *short gastrulation* to indicate lateral cell fate in *dorsal*-shRNA embryos. Green box indicates ventral side of embryo. *short gastrulation* expression across the entire ventral surface confirms expansion of lateral cell fate in lateralized embryos.

Figure S2. Phalloidin Injection Phenocopies Depletion Of F-Actin Disassembly Genes, Related To Figure 3. (A-C) Mean total apical F-actin levels (green line) and mean apical area (black line) of cells from embryos expressing the indicated UAS-shRNA and Utr::GFP (F-actin). Data shows representative embryo of n=3, averaging ~50 cells per condition. (D-H) Stabilizing F-actin by injecting AlexaFluor568-labeled phalloidin inhibits medioapical F-actin disassembly. Injected embryos are expressing Utr::GFP (F-actin). (D and F) Persistent F-actin foci are observed near the site of phalloidin injection (local). (D and G) Apical F-actin does not accumulate into foci farther away from injection (distal) or following vehicle injection (E). (H) Accumulation of medioapical F-actin is specific to apically constricting cells; in non-ventral cells (*Drosophila* germband) F-actin accumulates at spots on “vertical” junctions. (I and J) Time-lapse images of vehicle- or phalloidin-injected embryos expressing Sqh::GFP (MyoII) and Gap43::CHFP (subapical membrane). (I) In vehicle-injected embryos MyoII remains medioapical during apical constriction. (J) Following phalloidin injection MyoII structures become unattached from the junction and are displaced from the medioapical domain. Loss of the attachment between the contractile motor and junctions is restored and MyoII again becomes medioapical. Dots track MyoII foci. Scale bars; 5 μ m.

Figure S3. F-Actin Meshwork Holes Are Present Between Medioapical Contractile Domain And Junctions, Related To Figure 4. (A) Time-lapse images of embryos expressing ubi-ROCK::GFP (Rho kinase, ROCK) and Utr::CHFP (apical and subapical F-actin) revealed that F-actin meshwork holes (white arrowheads) form between ROCK foci (red arrow) and junctions. (B) Images of fixed *wild-type* embryos stained for Moesin used to measure bleb position. Supra-apical Moesin labels plasma membrane blebs, subapical Moesin labels cell periphery. (C) Schematic outlines quantitative analysis used to determine bias in bleb position. To determine the statistical significance of the positional enrichment of “actual” blebs, we generated a null distribution using randomly chosen points in the field of cells and measured distances to these points (Random). Scale bars; 5 μ m.

Figure S4. Slowed F-Actin Turnover Via Depletion Of Chic Or Cib Slows Filling Of F-Actin Meshwork Holes, Related To Figure 5. (A) Time-lapse images of representative cells from embryos expressing Utr::GFP (apical and subapical F-actin) and the indicated UAS-shRNA. F-actin meshwork holes are slower to fill (red arrow) and persist longer following Chic or Cib depletion. Scale bars; 5 μ m. (B) Box and whisker plot of hole persistence. Average duration of meshwork holes is increased following Chic or Cib depletion compared to *ctl*-shRNA. n=6 embryos, 10 F-actin meshwork holes per embryo for each condition. (C) Box and whisker plot of timing to reestablish force balance following an imbalance in mutants with slowed F-actin assembly. N=6 embryos, 10 holes per embryo for each condition. (D-F) Loss of actin monomer recycling via Chic and Cib depletion slows apical constriction and total apical F-actin intensity reduction. (D) Mean total apical F-actin levels (green line) and mean apical area (black line) of cells from embryos expressing Utr::GFP and the indicated UAS-shRNA. Data shows

representative embryo of n=3, averaging ~50 cells per condition. (E and F) Box and whisker plot of percent change in total apical F-actin level (E) and apical area reduction (F) 400 seconds after apical constriction onset following Chic or Cib depletion. Data represents n=3 embryos, ~50 cells per embryo for each condition. *** $p < 0.0001$, ** $p < 0.001$, * $p < 0.01$. n.s.= not significant.

Figure S5. Slowing F-Actin Turnover Does Not Disrupt Junctional E-Cadherin Localization, Related To Figure 6. (A) Embryos expressing indicated UAS-shRNA were fixed and stained for phalloidin (subapical F-actin, magenta) and E-cadherin (AJs, green). E-cadherin is restricted to junctions and present in punctate structures in F-actin turnover mutants, similar to *ctl-shRNA* embryos. Scale bars; 5 μ m. (B) Box and whisker plot showing the ratio of junctional E-cadherin expression versus medioapical E-cadherin expression following indicated gene depletion. Loss of F-actin turnover results in a slight decrease in junctional E-cadherin expression without increasing the medioapical pool. *** $p < 0.001$, ** $p < 0.01$, * $p < 0.02$. n.s. is not significant. (C) Time-lapse images of a Latrunculin B injected embryo expressing ubi-E-cadherin::GFP (E-cadherin) and Sqh::CHFP (MyoII). E-cadherin localization persists at the cell-cell interface (yellow arrow) during MyoII (white asterisks) separation and restoration of force balance. Red arrow indicates *de novo* MyoII that appears at junction during restoration of force balance. Scale bars; 5 μ m. (D and E) Cell outlines correspond with images in B. (D) Cell outline prior to (black line) and after MyoII separation (red dotted line), showing the movement of the cell-cell interface and opposing movement of MyoII (Arrow). (E) Cell outlines prior to (red solid line) and after restoration of force balance (blue dotted line) show the movement of MyoII and opposing interface toward the previously coupled interface.

Figure S6. Capt And Cib Localize To The Subapical Cytoplasm In Apically Constricting Cells, Related To Figure 7. (A and B) GFP::Capt localization in live embryos (A) and endogenous Capt localization in fixed embryos (B). In apically constricting ventral cells, GFP-Capt (A) and endogenous Capt (B) present diffusely in the subapical cytoplasm, but GFP::Capt becomes junctional in the non-ventral cells. (B) Endogenous Capt in *ctl-shRNA* embryos is lost in *capt-shRNA*, confirming specificity of the signal and knock down. (C) Cib::GFP is localized to the cytoplasm in ventral cells during apical constriction in fixed embryos. Scale bars; 5 μ m.

Table S1. Actomyosin Regulatory Genes Targeted in Live-Imaging RNAi Screen, Related to Figure 1. Actin regulators targeted in RNAi screen. Maternal driver and incubation temperature used to obtain viable embryos is indicated for each shRNA line.

Movie S1. Inhibiting F-actin Turnover Results in Unstable Force Balance in Tissue, Related To Figure 1. Indicated UAS-shRNA expressing Sqh::GFP (MyoII). Reduced F-actin turnover in *chic-shRNA* embryo results in a dynamic loss of force balance defined by abnormal back and forth movement of MyoII structures across the tissue. Loss of cortical anchoring in *cno-shRNA* embryo results in a permanent uncoupling of the contractile motor from AJ. Shown at 15 fps.

Movie S2. Latrunculin A and B Injection Phenocopies Depletion of F-Actin Turnover Proteins, Related to Figures 1. Sqh::GFP (MyoII) expressing embryos injected with vehicle only latrunculin A, or latrunculin B. Doses of latrunculin A or B were used that does not completely depolymerize F-actin. Latrunculin A and B injection results in a loss of force balance, similar to Chic depletion (see Movie S1). Shown at 15 fps.

Movie S3. Profilin (Chic) Depletion Results in Loss of Cell-Cell Adhesion and Failed Tissue Folding, Related to Figures 1. Indicated UAS-shRNA expressing Gap43::CHFP (membrane). Disrupting F-actin turnover causes cells to round up near the end of the movie, which is indicative of loss of cell adhesion. Shown at 15 fps.

Movie S4. Slingshot (Ssh) Depletion Results in Failed Tissue Folding, Related to Figures 3. Indicated UAS-shRNA expressing Utr::GFP (F-actin). Hindered F-actin disassembly eventually disrupts cell-cell adhesion and cells come back to the embryo surface rather than invaginating. Shown at 15 fps.

Movie S5. Dynamic F-actin Meshwork Holes Form During Apical Constriction, Related to Figure 4. *ctl-shRNA* embryo expressing fluorescent Utr::GFP (apical and subapical F-actin) shows dynamic meshwork rearrangement of apical F-actin (green) during apical constriction. Holes are formed in the F-actin meshwork, often proximal to junctions. Subapical F-actin (gray) labels cell periphery. Shown at 15 fps.

Movie S6. Inhibiting F-actin Turnover Results in Transient Loss of the Contractile Machinery's Attachment to Junctions, Related to Figure 5. Embryos expressing indicated UAS-shRNA and Sqh::GFP (MyoII, green) and Gap43::CHFP (plasma membrane, grayscale). Loss of F-actin turnover via Ssh or Cib depletion leads to the dynamic loss of force balance, resulting in the displacement of medioapical MyoII (yellow arrow). Force balance is subsequently repaired. Shown at 15 fps.

Movie S7. MyoII Recruitment to Detached Junction Prior to Repair, Related to Figure 6. Embryos expressing indicated UAS-shRNA and Sqh::GFP (MyoII, green) and Gap43::CHFP (plasma membrane, grayscale) show MyoII recruitment to cell-cell interface (red arrow) following force imbalance prior to its repair and the relocalization of the displaced medioapical MyoII (yellow arrows). Shown at 15 fps

SUPPLEMENTAL METHODS

Fly Stocks

The following maternal GAL4 drivers were used: [Mat67,Sqh::GFP;Mat15,Gap43CHFP], [Mat67;Mat15], [Mat67;Utr::GFP], [Sqh::GFP;Mat15,Gap43::CHFP], [Sqh::CHFP, Utr::GFP; Mat15]. *Spn27a-shRNA* and *Dorsal-shRNA* expression was driven by [Mat67;15] to induced ventralized and lateralized embryos, respectively in Figures 2C and S2. The following flies were used for live imaging or laser ablation experiments: [Utr::GFP], [Utr::CHFP;ubi-E-cadherin::GFP], [Utr::CHFP;Sqh::GFP], [Utr::CHFP;ubi-GFP::ROCK], [Utr::GFP;Gap43::CHFP], [Utr::Venus;Gap43::CHFP], [ubi-E-cadherin::GFP; SqhCHFP], [GFP::Ciboulot protein trap; (stock # 109708, Kyoto DGRC, Kyoto, Japan)]. Germ line clones are generated from [sqh¹,FRT101/FM7; P{w+,sqh-TS::GFP}attP1 P{w+ Gap43::mCherry}, attP40/CyO] and [sqh¹,FRT101/FM7; P{w+,sqh-AE::GFP}attP1 P{w+ Gap43::mCherry}, attP40/CyO], as described in Vasquez CG *et al.*, 2014. sqh-TS::GFP and sqh-AE::GFP transgenes were expressed via the endogenous sqh promoter. Germline clones were generated using the FLP-DFS technique by heat shocking mutant/ovoD larvae for 2 h at 37°C for 3–4 days (Chou and Perrimon, 1992). For sqh::GFP rescue of sqh¹ germline clones, sqh¹ FRT/FM7; sqh-XX::GFP/CyO females were crossed to ovoD FRT/Y; hsFlp males. The resulting larvae were heat shocked, and sqh¹ FRT/ovoD FRT; sqh-TS or AE::GFP/hsFlp females were crossed to OreR males to collect embryos that resulted from germline clones.

Microscopy

Live and fixed images were acquired on a Zeiss LSM 710 confocal microscope, with a 40×/1.2 Apochromat water objective (Zeiss), an argon ion, 561 nm diode, 594 nm HeNe, and 633 nm HeNe lasers. Pinhole settings ranged from 1–2 airy units. For two-color, live imaging, simultaneous excitation was used with band-pass filters set at ~499–561 nm for GFP and ~599–696 nm for CHFP. All images shown are representative of at least four embryos unless otherwise stated.

Live imaging- Embryos were dechorionated with 1:1 bleach/water for 2 minutes, washed with water, and mounted ventral side up onto a slide coated with embryo glue (double-sided tape soaked in heptane). Spacer coverslips (No. 1.5) were attached using glue and a coverslip was attached to create a chamber. Halocarbon 27 oil was added to the chamber. Embryos were not compressed. Imaging was performed at room temperature (~23 °C) on a Zeiss LSM 710 confocal microscope.

Fixed imaging- Embryos were dechorionated with 1:1 bleach and water solution for 2 minutes, washed with water, then fixed in 4% paraformaldehyde in 0.1 M phosphate buffer at pH 7.4 with 50% heptane for 30 min and manually devitellinized. To visualize F-actin, embryos were then incubated with Alexafluor488- or AlexaFluor568-conjugated phalloidin (Invitrogen, Carlsbad, CA) diluted in PBS+0.1% Triton X-100 (PBST) overnight (~12 hours) at 4°C. Embryos were then blocked with 10% BSA in PBST. Primary and secondary antibodies were diluted in 5% BSA in PBST. For cross-sections, embryos were post-fixed after antibody staining for 30 min before cutting. Embryos were then mounted ventral side up using AquaPolymount (Polysciences).

Live-embryo imaging RNAi screen- Virgin females carrying the UAS-shRNA were crossed to males carrying a maternal driver. Next, females carrying both the UAS-shRNA and the maternal driver were crossed to UAS-shRNA males, and resulting live embryos were imaged (see details below). A complete list of UAS-shRNA lines and their corresponding drivers used in the screen are in Table S1 (Ni *et al.*, 2011). The following fluorescent protein fusions were used: ubi-Ecad (Oda *et al.*, 1994), Utr::GFP (Rauzi *et al.*, 2010), ubi-GFP::ROCK (Bardet *et al.*, 2013),

Gap43CHFP (Martin et al., 2010), Sqh::GFP (Martin et al., 2009).

Scanning electron microscopy- Dechorionated embryos were fixed with 50% glutaraldehyde in 0.1M cacodylate buffer and 50% heptane for 25 min and manually devitellinized. Embryos were dehydrated by a gradual increase in EtOH concentration (50%, 75%, 95%, 100%). Dehydrated embryos are incubated with a 1:1 EtOH/Hexamethyldisilazane (HMDS) for 10 min, and then 100% HMDS for 10 min. Following TMS evaporation, embryos are mounted ventral side up. Metal coating was performed using Sputter Coating System (Hummer 6.2), and samples were imaged using Jeol 5600LV Scanning Electron Microscope (W. M. Keck Microscopy Facility, Cambridge, MA).

Image processing

Images were processed using MATLAB (MathWorks), Photoshop CS6 (Adobe Systems) and Fiji (<http://fiji.sc/wiki/index.php/Fiji>). Figures are prepared using Illustrator C6 (Adobe Systems). A Gaussian filter (kernel = 1 pixel) was applied to images. Apical images are maximum intensity projections of multiple z sections (~2–3 μm). Subapical images are one z slice, ~1–2 μm below the apical sections.

Laser ablation

Laser ablations were performed using a 2-photon Mai-Tai laser set to 800 nm on a LSM710 confocal microscope (Zeiss) through a 40x/1.1 objective, using the Zen software (Zeiss) (W. M. Keck Microscopy Facility, Cambridge, MA). For ablations, laser power was set at 20%, with a scan speed within the ROI of 0.08 ms/px. Ablations were performed within a linear ROI of 22 μm . The sqh::GFP or sqh::CHFP signal was used to visualize the opening of the apical actomyosin meshwork and GFP::ROCK was used to visualize ROCK.

Immunofluorescence

The following antibodies were used for immunofluorescence: anti-Capt (1:500, gift from Buzz Baum, MRC Laboratory for Cell Biology, London, England), anti-Neurotactin (BP106, 1:100, Developmental Studies Hybridoma Bank), anti-E-cadherin (Dcad2, 1:25, Developmental Studies Hybridoma Bank), Cofilin (Ab-3, 1:250, Signalway Antibody, College Park, MD), and Phospho-Cofilin (Phospho-Ser3, 1:250, Signalway Antibody), anti-Moesin (1:5000, gift from Sebastien Carreno, University of Montreal, Canada), and AlexaFluor488, 568 or 647 secondary antibodies were at 1:500 (Invitrogen; catalogue numbers A11034, A11036, A21245, A11031, A21235 and A21247). Fixed images were acquired on a Zeiss LSM 710 confocal microscope.

Immunoblotting

Protein extracts were prepared by homogenizing early gastrulating embryos in SDS sample buffer. Samples were run on 10% SDS-PAGE gels. Protein was transferred to 0.45- μm nitrocellulose membrane (Bio-Rad Laboratories) and the indicated primary antibodies were detected using horseradish peroxidase-labeled secondary antibodies (1:1,000, Jackson ImmunoResearch Laboratories, Inc.). The following antibodies were used to detect protein levels: anti-Capt (1:1,000, gift from Buzz Baum, MRC Laboratory for Cell Biology, London, England), anti-dPod-1 (1:1,000, gift from Yu Nung Jan, University of California San Francisco, San Francisco, CA), anti-Cofilin (Ab-3, 1:500, Signalway Antibody), anti-Phospho-Cofilin (Phospho-Ser3, 1:500, Signalway Antibody), anti-Zipper (1:1,000, gift from Eric Wieschaus, Princeton University, Princeton, NJ), anti-Ciboulot (1:3,000, gift from Thomas Preat, ENP, Paris, France), anti-Snail (1:1,000, gift from Mark Biggins, Lawrence Berkeley National Laboratory, Berkeley, CA), and anti-Diaphanous (1:1,000, gift from Stanley Wasserman, Indiana University Bloomington, Bloomington, IN). Tubulin (DM1a, 1:2,000, Sigma, St. Louis, MO) and anti-Actin (224-236-1, 1:1,000, Developmental Studies Hybridoma Bank, Iowa City, IA) were used as loading controls.

RNA Isolation, Reverse Transcription, and Real-Time qPCR

Detailed protocols are provided in the Extended Materials and Methods of (Sopko et al., 2014). Briefly, RNA was isolated by guanidinium thiocyanate-phenol-chloroform extraction using TRIzol (Life Technologies) and glass-bead-based cell disruption. DNase (QIAGEN) incubation eliminated genomic DNA. Samples were processed for cleanup with an RNeasy MinElute Cleanup Kit (QIAGEN). One microgram of purified RNA was incubated with a mix of oligo(dT) and random hexamer primers and with iScript RT (iScript cDNA Synthesis Kit, Bio-Rad) for complementary DNA (cDNA) synthesis. cDNA was used as the template for amplification, using validated primers in iQ SYBR Green Supermix with a CFX96 Real-Time PCR detection system (Bio-Rad). Query gene expression was relative to a control sample, normalized to the expression of three reference genes: *ribosomal protein L32*,

alpha-tubulin, and either *nuclear fallout* or *Gapdh1*, using the $\Delta\Delta C(t)$ analysis method.

shRNA Line Generation

Details on the individual shRNA lines used in this study can be found at <http://www.flyrnai.org/TRiP-HOME.html>. shRNAs were cloned in VALIUM vectors and injected into embryos at genomic attP landing sites on the second (attP40) or third (attP2) chromosomes as described in (Ni et al., 2011).

Generation of GFP::Capt

Using the Capt Bacterial Artificial Chromosome (BAC) CH322-128G03 (BACPAC Resource Center, Oakland, CA), Capt was amplified using the following primers- Capt Fwd: TGCCACTAAATTTGGGCCATA, Capt Rev: GCG AAT AGA TGG GGT GGT G, Capt Fwd + Neo Overhang: CGC CAT CAT CAC CAG GCC TTT GCA GGC GTG TGG C, and Capt Rev + Neo Overhang: CTT GAC GAG TTCT TCT GAT TCT CCT GCT GCC GAT C. GFP was inserted N-terminal to Capt ORF using the following primers- GFP Fwd: ATG GTG AGC AAG GGC GAG GAG, and GFP Rev: CTT GTA CAG CTC GTC CAT GCC. The resulting BACs were verified by sequencing of the recombined regions prior to phiC31-mediated integration at the attP2 on the 3rd chromosome. Transgenesis was performed by Rainbow Transgenics. Genomic rescue showed that GFP::Capt encodes fully functional versions of the Capt; homozygous *capt*^{E593} mutants carrying two copies of GFP::Capt are viable.

Drug injections

Embryos were dechorionated and mounted ventral side up then desiccated for 5 min (Drierite, Drierite Company, City, ST). 3:1 halocarbon 700/halocarbon 27 oils was added on the embryo for injection. Embryos were injected at one pole (end on injection) or laterally during mid-to-late cellularization (furrow canals at base of nuclei) for ventral furrow cells with a drop size of around 40 μ m, estimating a 1:200–300 dilution of the drug. Phalloidin (Enzo Life Sciences, Farmingdale, NY) was resuspended at 10mg/mL in MeOH. **Phalloidin Injection:** Alexafluor568-conjugated phalloidin (Invitrogen) is resuspended at ~600 μ g/mL in MeOH. A 1:5 mixture of Alexafluor-568-conjugated Phalloidin and unconjugated Phalloidin was injected at 300 μ g/mL. To assess F-actin behavior, 5 Utr::GFP expressing-embryos were injected and imaged; embryo in Figure S3D-H is a representative embryo. To assess force balance, 6 sqh::GFP- and Gap43::CHFP-expressing embryos were injected; embryo in Fig S3J is representative images. 7 embryos were vehicle injected (MeOH alone) as controls. All embryos are imaged ~3-5 minutes after injection. **Latrunculin A and B Injection:** Latrunculin A (Enzo Life Sciences, Farmingdale, NY) was resuspended at 5mg/mL in EtOH and injected at 150 μ g/mL. Latrunculin B (Enzo Life Sciences) was resuspended at 5mg/mL in EtOH and injected at 120 μ g/mL. These doses slows F-actin turnover without promoting F-actin depolymerization. For latrunculin A, 6 ubi-Ecad-GFP-expressing embryos and 7 sqh::GFP- and Gap43::CHFP-expressing embryos were injected and imaged and embryo in Figure S6B and Movie S2 are representative images. For latrunculin B, 9 sqh::GFP- and Gap43::CHFP-expressing embryos were injected and imaged and embryo in Movie S2 is a representative image. 9 embryos were vehicle injected (EtOH alone) as controls. All embryos are imaged ~3-5 minutes after injection. For experiments in Figure 1G, at least 8 *ctl-shRNA* and *zip-shRNA* embryos expressing sqh::GFP and Gap43::CHFP were injected with vehicle alone (EtOH) or latrunculin B.

SUPPLEMENTAL REFERENCES

Chou, T.B., and Perrimon, N. (1992). Use of a yeast site-specific recombinase to produce female germline chimeras in *Drosophila*. *Genetics* *131*, 643-653.

Ni, J.Q., Zhou, R., Czech, B., Liu, L.P., Holderbaum, L., Yang-Zhou, D., Shim, H.S., Tao, R., Handler, D., Karpowicz, P., et al. (2011). A genome-scale shRNA resource for transgenic RNAi in *Drosophila*. *Nature methods* *8*, 405-407.

Oda, H., Uemura, T., Harada, Y., Iwai, Y., and Takeichi, M. (1994). A *Drosophila* homolog of cadherin associated with armadillo and essential for embryonic cell-cell adhesion. *Developmental biology* *165*, 716-726.

Sopko, R., Foos, M., Vinayagam, A., Zhai, B., Binari, R., Hu, Y., Randklev, S., Perkins, L.A., Gygi, S.P., and Perrimon, N. (2014). Combining genetic perturbations and proteomics to examine kinase-phosphatase networks in *Drosophila* embryos. *Developmental cell* *31*, 114-127.